Half-life and initial Solar System abundance of ^{146}Sm determined from the oldest andesitic meteorite

Linru Fang[a,1] ⓘ, Paul Frossard[b], Maud Boyet[b], Audrey Bouvier[c] ⓘ, Jean-Alix Barrat[d,e] ⓘ, Marc Chaussidon[a] ⓘ, and Frederic Moynier[a,1] ⓘ

The formation and differentiation of planetary bodies are dated using radioactive decay systems, including the short-lived ^{146}Sm-^{142}Nd ($T_{1/2}$ = 103 or 68 Ma) and long-lived ^{147}Sm-^{143}Nd ($T_{1/2}$ = 106 Ga) radiogenic pairs that provide relative and absolute ages, respectively. However, the initial abundance and half-life of the extinct radioactive isotope ^{146}Sm are still debated, weakening the interpretation of ^{146}Sm-^{142}Nd systematics obtained for early planetary processes. Here, we apply the short-lived ^{26}Al-^{26}Mg, ^{146}Sm-^{142}Nd, and long-lived ^{147}Sm-^{143}Sm chronometers to the oldest known andesitic meteorite, Erg Chech 002 (EC 002), to constrain the Solar System initial abundance of ^{146}Sm. The ^{26}Al-^{26}Mg mineral isochron of EC 002 provides a tightly constrained initial δ^{26}Mg* of -0.009 ± 0.005 ‰ and (^{26}Al/^{27}Al)$_0$ of $(8.89 \pm 0.09) \times 10^{-6}$. This initial abundance of ^{26}Al is the highest measured so far in an achondrite and corresponds to a crystallization age of 1.80 ± 0.01 Myr after Solar System formation. The ^{146}Sm-^{142}Nd mineral isochron returns an initial ^{146}Sm/^{144}Sm ratio of 0.00830 ± 0.00032. By combining the Al-Mg crystallization age and initial ^{146}Sm/^{144}Sm ratio of EC 002 with values for refractory inclusions, achondrites, and lunar samples, the best-fit half-life for ^{146}Sm is 102 ± 9 Ma, corresponding to the physically measured value of 103 ± 5 Myr, rather than the latest and lower revised value of 68 ± 7 Ma. Using a half-life of 103 Ma for ^{146}Sm, the ^{146}Sm/^{144}Sm abundance of EC 002 translates into an initial Solar System ^{146}Sm/^{144}Sm ratio of 0.00840 ± 0.00032, which represents the most reliable and precise estimate to date and makes EC 002 an ideal anchor for the ^{146}Sm-^{142}Nd clock.

meteorite | Sm-Nd | early Solar System | Erg Chech 002

The timescales of formation and differentiation of the early Earth (i.e., the Hadean period) and the Moon as well as terrestrial planets such as Mars are essential to generally understand the origin and evolution of planetary bodies (1). Various isotopic chronometers (e.g., U-Pb, Sm-Nd, Lu-Hf, Hf-W, and I-Pu-Xe) provide broad constraints on early differentiation processes such as core segregation, mantle stratification, and atmospheric and crust formation, and the extinct radionuclides are powerful tracers for the first million years of the Solar System (2–4). Among these systems, the rare-earth elements Sm and Nd play a unique role in geochemistry because they combine both short- (^{146}Sm-^{142}Nd), and long-lived (^{147}Sm-^{143}Nd) alpha decay systems. The short-lived ^{146}Sm-^{142}Nd decay system was active during the Hadean Era (>4 Ga). Therefore, measurements of ^{142}Nd/^{144}Nd were used to calculate model ages for the Earth's mantle-crust differentiation (5, 6) and to determine the age of crystallization of the martian and lunar magma oceans (7–9). However, the significance of the ages obtained using this method is limited by the disputed estimates of the half-life and the initial Solar System abundance of ^{146}Sm.

The ^{146}Sm isotope is a pure p-process radionuclide that is possibly produced by the supernova of Type Ia events in the early Solar System (10). There are only four determinations of the half-life of ^{146}Sm by particle counting experiments reported, with errors that show a range of values from 68 to 103 Ma (11–14). The latest determination at 68 ± 7 (1σ) Ma (14) is about a third shorter than the previously used value of 103 ± 5 Ma (12, 13), which casts further doubts on using ^{146}Sm-^{142}Nd systematics to obtain accurate timescales of early planetary differentiation processes. Each counting experiment may have possible systematic errors, making a consensus difficult to reach (15). For example, the different half-lives proposed for ^{146}Sm result in differences of up to 100 Myr for magmatic events that occurred toward the end of the Hadean eon (4). Furthermore, the large variation of the ^{146}Sm half-life weakens the potential for back-calculating the ^{146}Sm/^{144}Sm ratios of the initial Solar System using achondrites such as eucrites and angrites based on their absolute ages and ^{146}Sm abundance (14, 16). Nowadays, the widely used Solar System initial ^{146}Sm/^{144}Sm ratio (0.00828 ± 0.00044), on which all calculated ages are anchored, is currently based on data obtained on mineral separates from calcium-aluminum–rich refractory inclusions (CAIs) from carbonaceous (CC)

Significance

^{146}Sm-^{142}Nd radioactive systematics can provide constraints on the timing of early differentiation processes on Earth, Moon, and Mars. The uncertainties related to the initial abundance and half-life of the extinct isotope ^{146}Sm impede the interpretation of the ^{146}Sm-^{142}Nd systematics of planetary materials. The accurate determinations of Sm, Nd, and Mg isotopic compositions of the oldest "andesitic" achondrite Erg Chech 002 (EC 002) define a crystallization age of 1.8 Myr after the formation of the Solar System and provide the most accurate and reliable initial ratio of ^{146}Sm/^{144}Sm for the Solar System at 0.00840 ± 0.00032 using a ^{146}Sm half-life of 103 Ma, making EC 002 an anchor for ^{146}Sm-^{142}Nd systematics for Earth and planetary materials.

chondrites (17). However, the Allende Al3S4 CAI, on which the initial $^{146}Sm/^{144}Sm$ was estimated, has not been dated by Al-Mg or Pb-Pb systems. Besides, it has a much younger Rb-Sr age of 4247 ± 110 Ma (17) than the reported Pb-Pb absolute ages of different refractory solids (18–20) and thus might have been modified by secondary processes and may not represent the earliest reservoir of the Solar System. Additionally, the radiogenic contribution to ^{142}Nd might be compromised by nucleosynthetic anomalies (21, 22). In particular, the different mineral fractions analyzed in Allende Al3S4 CAI exhibit large and variable ^{148}Nd and ^{150}Nd anomalies (17), questioning the accuracy of the measured $^{142}Nd/^{144}Nd$ ratios and the validity of the deduced initial $^{146}Sm/^{144}Sm$.

Erg Chech 002 (EC 002) is a unique silica-rich achondrite recognized as the oldest primordial crust sample discovered to date, with an estimated crystallization age of 2.255 ± 0.013 Myr after CAI formation obtained using in situ secondary ion mass spectrometry (SIMS) ^{26}Al-^{26}Mg measurements (23). The abundance of coarse crystals of pyroxene and plagioclase in EC 002 makes it possible to separate minerals with fractionated Sm/Nd ratios. Given its old reported age, large variations in ^{142}Nd abundances are expected. Altogether, these characteristics make EC 002 a suitable igneous sample to estimate the ^{146}Sm half-life and to establish the initial $^{146}Sm/^{144}Sm$ Solar System ratio by comparing its isotopic systematics with those of other asteroidal and planetary objects. Furthermore, the measurement of mass-independent Nd stable isotope ratios may be used to identify whether the EC 002 parent body is of CC or noncarbonaceous (NC) chondritic source (22, 24–26) and therefore helps to obtain more insights into the origin of EC 002.

In this study, we report the Sm and Nd isotopic compositions of mineral fractions, leachates, and bulk samples of EC 002, as well as a high-precision internal ^{26}Al-^{26}Mg isochron obtained on the same mineral fractions. A robust crystallization age for EC 002 is constrained by ^{26}Al-^{26}Mg and ^{147}Sm-^{143}Nd mineral isochrons. Literature $^{146}Sm/^{144}Sm$ data of CAIs and asteroidal and planetary bodies are then combined with the $^{146}Sm/^{144}Sm$ value of EC 002 to obtain the best fit value for the half-life of ^{146}Sm. Finally, the ^{146}Sm-^{142}Nd isochron of EC 002 is used to deduce a precise and best estimate for the initial $^{146}Sm/^{144}Sm$ ratio of the Solar System.

Results

The Sm and Nd isotopic data and $^{144}Sm/^{144}Nd$ and $^{147}Sm/^{144}Nd$ ratios are reported in *SI Appendix*, Tables S1.1–S1.5. Neutron capture effects caused by galactic cosmic rays are significant for this meteorite as evidenced by the Sm isotopic composition of the bulk rock ($\varepsilon^{149}Sm = -5.81 \pm 0.05$, $\varepsilon^{150}Sm = 10.46 \pm 0.06$). Therefore, all the measured Nd isotopic ratios were corrected for neutron capture effects using the method of Borg et al. (9) and the measured Sm isotope composition of EC 002. The corrections on $\mu^{142}Nd$, $\mu^{143}Nd$, $\mu^{145}Nd$, $\mu^{148}Nd$ ($\mu^x Nd = \{(^x Nd/^{144}Nd)_{sample}/(^x Nd/^{144}Nd)_{standards} - 1\} \times 10^6$ in parts per million [ppm], with x = 142, 143, 145, or 148) are 2.5, 5.4, 3.9, and 0.7 ppm, respectively. After the neutron capture corrections, the two measured bulk-rock fractions provide an average $\mu^{145}Nd$ and $\mu^{148}Nd$ of 8.9 ± 2.5 (2SD) and 12.0 ± 3.6 (2SD) ppm, respectively. The ranges of $^{147}Sm/^{144}Nd$ and $^{143}Nd/^{144}Nd$ ratios of 15 EC 002 fractions are 0.1282 to 0.2349 and 0.510733 to 0.513784, respectively. The ^{147}Sm-^{143}Nd isochron (*SI Appendix*, Fig. S2, mean square of weighted deviation [MSWD] = 130) returns an initial $^{143}Nd/^{144}Nd$ ratio of 0.50679 ± 0.00018. An initial $\varepsilon^{143}Nd$ value of 0.43 ± 0.83 is calculated using the chondritic uniform reservoir

(CHUR) parameters of Bouvier et al. (27) and the method referred by Fletcher and Rosman (28). We note that the separation "D < 2.9 L (leachate of the mineral fraction D < 2.9)" falls off the correlation line for $^{143}Nd/^{144}Nd$ and $^{142}Nd/^{144}Nd$ ratios as defined by the seven other fractions (*SI Appendix*, Fig. S3), which might be due to its low Nd content; therefore, we excluded it from the rest of the discussion for the ^{146}Sm-^{142}Nd system. The range of $^{142}Nd/^{144}Nd$ ratios of seven fractions of EC 002 was 1.141726 to 1.141880, and all $^{144}Sm/^{144}Nd$ and $^{142}Nd/^{144}Nd$ ratios defined a regression line (Fig. 1, MSWD = 0.99) with an initial $^{142}Nd/^{144}Nd$ ratio of 1.141479 ± 0.000013 ($\mu^{142}Nd_0 = -17 \pm 11$ ppm, compared to the terrestrial standard JNdi-1) and a $^{146}Sm/^{144}Sm$ ratio of 0.00830 ± 0.00032.

The Mg isotopic data and $^{26}Al/^{24}Mg$ ratio are reported in *SI Appendix*, Table S2 for six separated fractions and one bulk sample. The $^{27}Al/^{24}Mg$ ratios ranged from 0.18 to 83.81, and the radiogenic ^{26}Mg excesses ($\delta^{26}Mg^* = \delta'^{26}Mg - \delta'^{25}Mg/\beta$, where $\delta'^x Mg = Ln[(^x Mg/^{24}Mg)_{sample}/(^x Mg/^{24}Mg)_{standards}] \times 1000$, x = 25 or 26; $\beta = 0.521$) ranges from 0.009 ± 0.011 to 5.257 ± 0.015 ‰. The linear correction between $\delta^{26}Mg^*$ and $^{27}Al/^{24}Mg$ (Fig. 2) defines an initial $^{26}Mg/^{24}Mg$ ratio ($\delta^{26}Mg^*_0$) of −0.009 ± 0.005 ‰ (2σ) and a slope corresponding to a $(^{26}Al/^{27}Al)_0$ of (8.89 ± 0.09) × 10^{-6}. Using the half-life of ^{26}Al of 0.705 Myr (29) and the $(^{26}Mg/^{24}Mg)_{standard} = 0.13932$ (30), the $(^{26}Al/^{27}Al)_0$ ratio of EC 002 corresponded to an age of 1.80 ± 0.01 Myr after CAIs formation using the initial $^{26}Al/^{27}Al$ ratio defined by CAIs [5.23 × 10^{-5} (18)].

Discussion

EC 002 is the oldest andesitic achondrite recognized to date based on an initial $^{26}Al/^{27}Al$ ratio of (5.72 ± 0.07) × 10^{-6} determined from ion microprobe analyses of crystals of plagioclase and pyroxene exposed in a polished section of EC 002 (23). The isochron obtained from multicollector inductively coupled plasma mass spectrometer (MC-ICP-MS) analyses of separated minerals (pyroxenes and plagioclases) yielded a slightly steeper slope corresponding to an initial $^{26}Al/^{27}Al$ ratio of (8.89 ± 0.09)×10^{-6}
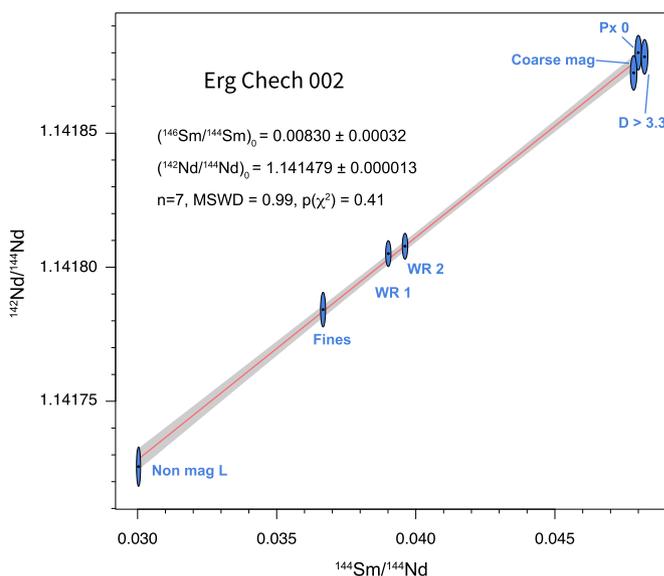
Fig. 1. ^{146}Sm-^{142}Nd mineral and bulk-rock isochron defined by seven mineral, leachate, and bulk fractions of the EC 002. The slope corresponds to $(^{146}Sm/^{144}Sm)_0 = 0.00830 \pm 0.00032$ (2σ) and the intercept of 1.141479 ± 0.000013 (2σ) as initial $^{142}Nd/^{144}Nd$ ($\mu^{142}Nd_0 = -17 \pm 11$ ppm, compared to the terrestrial standard JNdi-1). L, leachate. The detailed annotations of the fraction names can be found in *SI Appendix*.
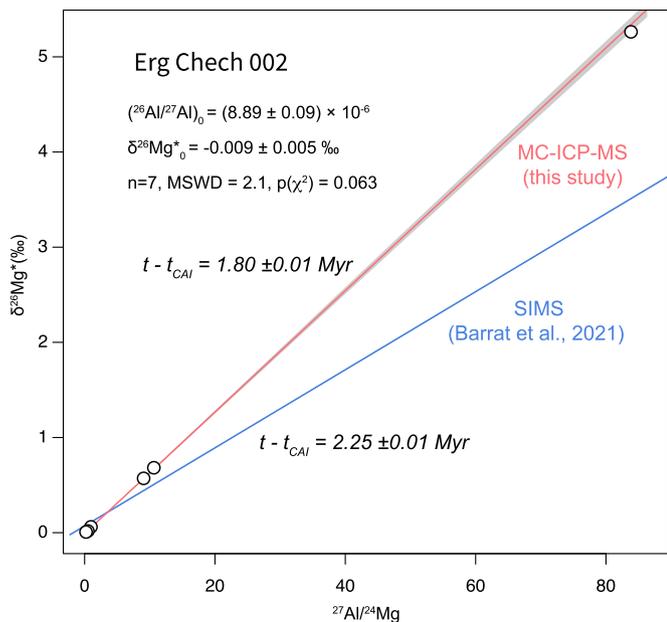
Fig. 2. ^{26}Al-^{26}Mg mineral and bulk-rock isochron defined by plagioclase, pyroxene, and bulk-rock fractions of the EC 002 meteorite (red line). The slope and the intercept of the isochron provide an initial $(^{26}Al/^{27}Al)_0$ ratio of $(8.89 \pm 0.09) \times 10^{-6}$ (2σ) and $\delta^{26}Mg\star_0 = -0.009 \pm 0.005$ ‰, (2σ), respectively. When anchored to the "canonical" initial Solar System $^{26}Al/^{27}Al$ ratio of 5.23×10^{-5} (18), we obtained an age of 1.80 ± 0.01 Myr. The ^{26}Al-^{26}Mg isochron defined by in situ SIMS measurements is plotted for comparison (blue line). The slightly steeper slope from this study corresponds to an ~450,000-y-older crystallization age for EC 002 compared to the age reported in Barrat et al. (23).

(Fig. 2). This gives an age ~450,000 y older than that of Barrat et al. (23). Furthermore, the $\delta^{26}Mg\star_0$ (initial $^{26}Mg/^{24}Mg$ ratio) calculated here (-0.009 ± 0.005 ‰) is slightly lower than in Barrat et al. (23) (0.065 ± 0.080 ‰), while consistent within uncertainty but more precise. The small discrepancy between these two datasets cannot result from systematic analytical errors. To reconcile the two datasets, the error should be ~120 ‰ on the $\delta^{26}Mg\star$ measured by ion probe on plagioclase with $^{27}Al/^{24}Mg \approx 5,000$, or alternatively, the error on the $^{27}Al/^{24}Mg$ ratio should be larger than 1,500 with $\delta^{26}Mg\star \approx 200$ ‰. Most likely, the two isochrons date two different events. This might be possible because of the much faster diffusion of Mg in plagioclase than in pyroxene [~5 orders of magnitude faster; e.g., (31, 32)]. Thus, the core of the plagioclase crystal analyzed by ion microprobe is likely not a closed system for Mg diffusion, contrary to the plagioclase-rich fractions analyzed by MC-ICP-MS (see *SI Appendix* for detailed discussion). In this hypothesis, the MC-ICP-MS ^{26}Al age would be closer to the crystallization age and will be used in the following discussion.

As a whole, we confirmed here that EC 002 is the oldest magmatic achondrite of the Solar System and that the small age difference based on two $^{26}Al/^{27}Al$ ratio estimates had no consequences for the discussion of the ^{146}Sm-^{142}Nd systematics. In addition, the initial distribution of ^{26}Al is debated to be either homogeneous with a "canonical" value of ~5×10^{-5} estimated from CAIs (18, 33) or to be heterogeneous with an initial ratio of ~1 to 2×10^{-5} for the forming region of some groups of chondrules and the angrite parent body (34, 35). Using the two potential initial $^{26}Al/^{27}Al$ ratios, the $^{26}Al/^{27}Al$ ratio of EC 002 translates into an age of 1.80 ± 0.01 Myr [anchored to a value of 5.23×10^{-5} (18)] or of 0.43 ± 0.01 Myr [anchored to a reduced value of 1.36×10^{-5} (34)] after the formation of the Solar System [$T_0 = 4,567.30 \pm 0.16$ Ma (20)]. Therefore, the absolute crystallization age of EC 002

could be considered to be between 4,565.5 and 4,566.9 Ma. However, such a small age range (<1.5 Myr) can only cause an ~1% variation on the ^{146}Sm initial abundance and half-life (much less than the error) and is thus insignificant for this study. Therefore, a crystallization age of 1.80 ± 0.01 Myr after CAIs, obtained using an initial $^{26}Al/^{27}Al$ ratio of 5.23×10^{-5} as Barrat et al. (23) did, is used in the rest of the discussion.

The fundamental dichotomy between NC and CC chondrite groups, which supposedly reflect a difference between inner and outer Solar System materials, has been established based on elementary and isotopic anomalies of Cr, Ti, Mo, and other elements (36–39). Recently it has been found that chondrites and achondrites from NC and CC Reservoirs have different Nd isotopic compositions with a small but resolvable Nd isotopic "gap" (22, 25, 26). EC 002 displays a $\mu^{145}Nd$ and $\mu^{148}Nd$ nucleosynthetic composition of 8.9 ± 2.5 (2SD) and 12.0 ± 3.6 (2SD) ppm, respectively. The $\mu^{148}Nd$ value of EC 002 is distinctly lower than any CC meteorite (Fig. 3) and falls within the NC region as other differentiated planetesimals such as angrite and eucrite parent bodies. This suggests that the parent body of EC 002 is likely derived from the NC meteorite reservoir. This conclusion is consistent with the fact that the negative Tm anomaly of the bulk EC 002 sample is similar to NC chondrites and achondrites (23).

The 15 mineral and bulk fractions of EC 002 define a ^{147}Sm-^{143}Nd age of $4,521 \pm 152$ Ma, which is consistent despite its large uncertainty with its corresponding Al-Mg age. The initial $\varepsilon^{143}Nd$ value of 0.43 ± 0.83 suggests that EC 002 is derived from a chondritic source. The slope and the intercept of $^{144}Sm/^{144}Nd$ and $^{142}Nd/^{144}Nd$ ratios defined by the seven mineral fractions and bulk samples correspond to an initial $^{146}Sm/^{144}Sm$ and $^{142}Nd/^{144}Nd$ of 0.00830 ± 0.00032 and 1.141479 ± 0.000013, respectively (Fig. 1). The precise Al-Mg age and $^{146}Sm/^{144}Sm$ ratio of the EC 002 parent body can be used to constrain the initial Solar System $^{146}Sm/^{144}Sm$ ratio, which, however, is strongly affected by two very different half-lives used in the scientific community [68 and 103 Ma (15)]. On the basis of the same set of data from achondrites (eucrite, mesosiderite, and angrite), the initial Solar System $^{146}Sm/^{144}Sm$ values were estimated as 0.0094 ± 0.0005 (14) or 0.0085 ± 0.0007 (49) using the ^{146}Sm half-life of 68 and 103 Ma, respectively. Moreover, the large differences of the ^{146}Sm half-life estimate not only hinder the reliability of the initials but also impede the potential of ^{146}Sm-^{142}Nd systematics for early Solar System chronology. Therefore, we provide an independent method using the coupled fit lines of crystallization ages from other robust dating systems (^{147}Sm-^{143}Nd, Pu-Xe, Pb-Pb, and ^{26}Al-^{26}Mg; see *SI Appendix*, Table S3 for details) and $^{146}Sm/^{144}Sm$ ratios of the meteorites, as well as the evolution trends of $^{146}Sm/^{144}Sm$ back-calculated from EC 002 to estimate the value of the ^{146}Sm half-life. The temporal evolution line of the $Ln(^{146}Sm/^{144}Sm)$ ratio (Fig. 4) is modeled with the slope ($-\lambda$, where λ represents decay constant) corresponding to either a ^{146}Sm half-life of 103 Ma or 68 Ma and a certain point constrained by EC 002 (Age = 1.80 Ma and $Ln(^{146}Sm/^{144}Sm) = -4.79$). In Fig. 4, the $Ln(^{146}Sm/^{144}Sm)$ ratios and ages of CAIs and achondrites are plotted together. All the points, especially the young lunar samples, fall closer to the evolution trend based on the ^{146}Sm half-life of 103 Ma (12, 13) compared to that of 68 Ma (14) (Fig. 4). Using all the scatters, we further defined the best fit curve and its confidence interval based on regression fitting. For the regression calculation, we converted the $^{146}Sm/^{144}Sm$ ratios of CAIs, achondrites, and lunar samples to $Ln(^{146}Sm/^{144}Sm)$, which we
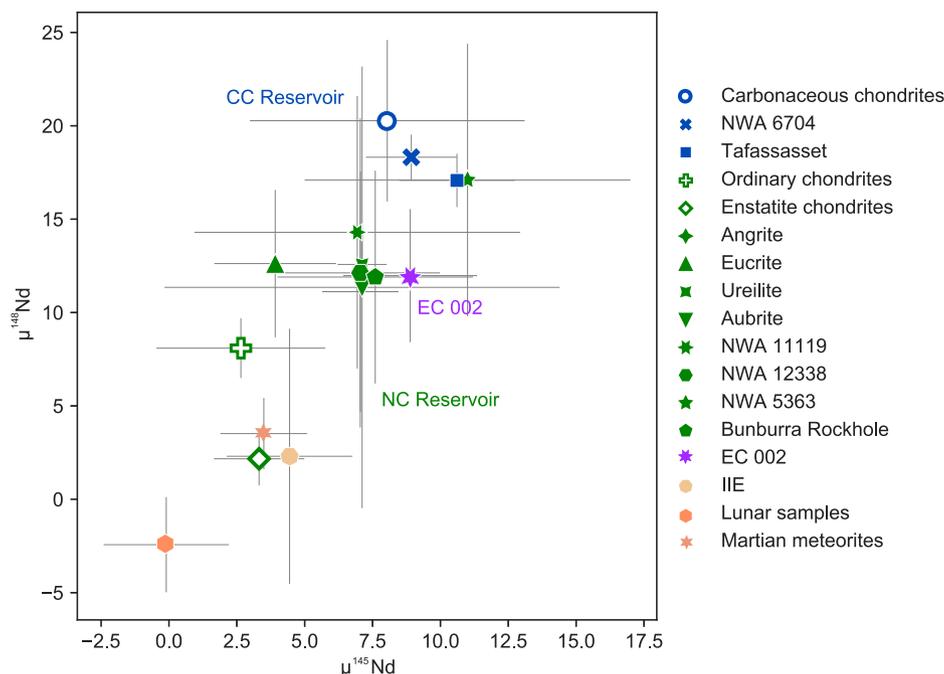
Fig. 3. μ^{145}Nd-μ^{148}Nd compositions of EC 002 compared with the mean compositions of chondrite groups (22, 24, 25, 40), achondrite groups (22, 26, 40, 41), lunar samples (3, 9, 42–44), and martian meteorites (26, 40, 45–48). Compiled μ^{145}Nd and μ^{148}Nd of meteorite groups and planetary bodies are from Frossard et al. (26). CC chondrites and achondrites (NWA 6704 and Tafassasset) have generally higher ^{148}Nd compared to inner Solar System and NC materials (26). EC 002 falls within the range of the NC Reservoir and also within the group of achondrite parent bodies (the outlier NWA 5363 has large errors) formed within 1.5 Myr after CAIs (26).

assumed to be linearly correlated with their ages [taking the Solar System age as $T_0 = 4,567.3$ Ma (20)]. The linear regression of the values and errors of Ln(^{146}Sm/^{144}Sm) and ages gives a slope of -0.00680 ± 0.00061 and an intercept of -4.80 ± 0.03 (Ln(^{146}Sm/^{144}Sm) $_{initial}$) using the IsoplotR Model 3 (50). The slope translates to the best fit line passing through all the data points (Fig. 4) fit to a half-life of 102 ± 9 Ma (95% confidence interval), providing robust support for the experimentally determined ^{146}Sm half-life value of 103 Ma, which is 35 Myr longer than the most recent determination (14). The combination of different radioactive systematics in CAIs, asteroidal, and planetary samples of various origins provides consistent results and an independent constraint on the half-life. It is important to stress the significance of the lunar samples (17) in the determination of the correct half-life, as the very ancient samples such as EC 002 actually work as an end-member for a more precise constraint in this approach (Fig. 4). The 35-Myr difference in the ^{146}Sm half-life affects the age of the early mantle differentiation and the age of differentiation of the lunar magma ocean (e.g., 9, 51) by over 100 Myr (52). Using the 103-Ma half-life confirmed here eliminates a large source of uncertainty of these age determinations.

By combining the ^{26}Al-^{26}Mg crystallization age of EC 002 of 1.80 ± 0.01 Myr after CAI formation with the ^{146}Sm/^{144}Sm abundance recorded by the same mineral fractions, we deduced an initial ^{146}Sm/^{144}Sm for the Solar System of 0.00840 ± 0.00032 and the temporal evolution curve of ^{146}Sm abundance (*SI Appendix*, Fig. S4) using the ^{146}Sm half-life of $103 \pm$ Ma (12, 13). This initial Solar System ^{146}Sm/^{144}Sm value is consistent within error with previous estimates such as the ones determined from eucrites of 0.0084 ± 0.0005 ($T_{1/2} = 103$ Ma) (49), a combination of eucrites and angrites of 0.0085 ± 0.0005 ($T_{1/2} = 103$ Ma) (16), and Allende CAI Al3S4 of 0.00828 ± 0.00044 (17), albeit with better precision. Moreover, our ^{146}Sm/^{144}Sm value corresponds to (^{146}Sm/^{144}Sm)$_{initial}$ of 0.0082 ± 0.0003 of the

fitted line (Fig. 4), which is compiled using the most reliable coexisting ages and ^{146}Sm-^{142}Nd data of various extraterrestrial samples. The consistency of the initial ^{146}Sm abundance estimated from different meteorite materials supports the previous suggestions (16, 49) that the distribution of ^{146}Sm was homogeneous in the early Solar System, at least for the CAIs and NC-forming regions. The initial Solar System ^{146}Sm/^{144}Sm abundance of 0.00840 ± 0.00032 deduced from EC 002 is therefore the most reliable and precise estimate to use for ^{146}Sm-^{142}Nd chronology.

In conclusion, we obtained ^{26}Al-^{26}Mg and ^{146,147}Sm-^{142,143}Nd mineral internal isochrons for the EC 002 ungrouped achondrite meteorite. The Al-Mg systematics confirmed that EC 002 is the oldest andesitic meteorite with a formation age at 1.80 ± 0.01 Myr after the Solar System formation [when anchored to an initial ^{26}Al/^{27}Al ratio of 5.23×10^{-5} (18)]. Stable Nd isotopic anomalies indicate that the parent body of EC 002 formed within the NC Reservoir, in agreement with the negative Tm anomaly displayed by the whole rock (23). By combining chronological records with the ^{146}Sm-^{142}Nd systematics of extraterrestrial samples formed within the first 200 Myr of Solar System history [especially lunar samples formed at 4.30 to 4.36 Ga (9, 51)], we confirmed that the most consistent half-life of ^{146}Sm is 103 Ma. Using this half-life, the formation age of EC 002, and the ^{146}Sm/^{144}Sm mineral isochron slope, we deduced a ^{146}Sm/^{144}Sm initial Solar System ratio of 0.00840 ± 0.00032. In association with its large recovered mass (~32 kg), abundant coarse mineral grains, and trace element–enriched composition, EC 002 represents the best anchor for ^{146}Sm-^{142}Nd systematics in planetary materials and possibly for other short-lived radioactive decay systems.

Materials and Methods

A mass of ~4 g of EC 002 was crushed in an agate mortar dedicated to meteorite work, from which several mineral and bulk-rock fractions were separated. Thirteen of them (seven mineral fractions and six leachates) in addition to two bulk-rock powders were analyzed for Sm and Nd isotope compositions. We
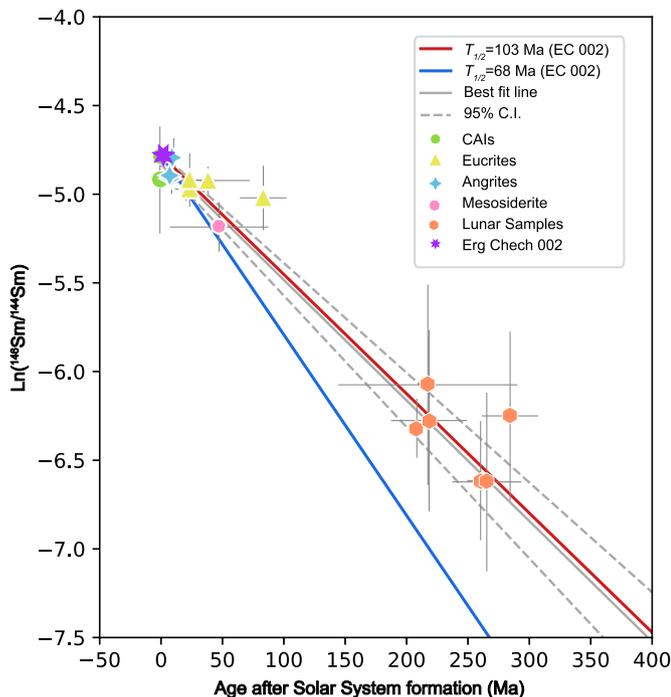
Fig. 4. Temporal evolution trend of the Ln(^{146}Sm/^{144}Sm) ratios using Ln(^{146}Sm/^{144}Sm) and age of EC 002 with a ^{146}Sm half-life of 68 Ma (blue line) and of 103 Ma (red line). For comparison, data for CAIs, eucrites, angrites, mesosiderite, and lunar samples (*SI Appendix*, Table S2 for further information) are reported. Using the linear correlation between Ln(^{146}Sm/^{144}Sm) and corresponding ages of these meteorites, the IsoplotR Model3 (50) provides the slope and intercept with respective errors for the best fit line (gray solid line) and its 95% confidence interval (95% C.I., gray dashed lines), corresponding to a fitted ^{146}Sm half-life value and Solar System initial ^{146}Sm/^{144}Sm ratio of 102 ± 9 Ma and 0.0082 ± 0.0003, respectively.

measured unspiked isotope compositions for stable Sm, Nd, and radiogenic Nd isotopic ratios and used the isotope dilution method for determining precisely the ^{147}Sm/^{144}Nd of all the fractions [following the splitting method detailed in Bouvier and Boyet (21)]. Among these samples, eight fractions with high Nd contents were analyzed for Nd isotopic compositions independently once again. Six mineral fractions and one bulk rock were analyzed for their Al-Mg isotopic compositions. The mineral fractions were separated using a combination of hand magnet, magnetic separator, and heavy liquids of the density of 2.9 and 3.3 (see *SI Appendix* for details). In addition, three widely available terrestrial samples (United States Geological Survey, basalt BHVO-2, BCR-2, and andesite AGV-2) were also analyzed to monitor data quality. All the fractions were passed through columns with ion exchange and specific resins in several steps to discard matrix and purify solutions for Nd and Mg (see details in *SI Appendix*). Neodymium and Sm isotope compositions were analyzed at the Laboratoire Magmas et Volcans, and detailed methods can be found in the *SI Appendix*. The Mg isotopic composition and ^{27}Al/^{24}Mg ratio were analyzed at the Institut de Physique du Globe de Paris (IPGP) following the method described in the *SI Appendix*. Both ^{146}Sm-^{142}Nd, ^{147}Sm-^{143}Nd and ^{26}Al-^{26}Mg internal isochrons were calculated using IsoplotR, Model1 (50).

Data Availability. The data have been deposited in a publicly accessible database, Mendeley Data, https://data.mendeley.com/datasets/kg78j55jpg/1.

1. S. B. Jacobsen *et al.*, Isotopes as clues to the origin and earliest differentiation history of the Earth. *Philos. Trans.- Royal Soc., Math. Phys. Eng. Sci.* **366**, 4129–4162 (2008).
2. T. Kleine, C. Münker, K. Mezger, H. Palme, Rapid accretion and early core formation on asteroids and the terrestrial planets from Hf-W chronometry. *Nature* **418**, 952–955 (2002).
3. M. Boyet, R. W. Carlson, L. E. Borg, M. Horan, Sm–Nd systematics of lunar ferroan anorthositic suite rocks: Constraints on lunar crust formation. *Geochim. Cosmochim. Acta* **148**, 203–218 (2015).
4. R. W. Carlson, M. Boyet, J. O'Neil, H. Rizo, R. J. Walker, "Early differentiation and its long-term consequences for Earth evolution" in *The Early Earth: Accretion and Differentiation*, J. Badro, M. Walter, Eds. (American Geophysical Union/John Wiley & Sons, Hoboken, NJ, 2015) 10.1002/9781118860359.ch8, pp. 143–172.
5. M. Boyet *et al.*, ^{142}Nd evidence for early Earth differentiation. *Earth Planet. Sci. Lett.* **214**, 427–442 (2003).
6. G. Caro, B. Bourdon, J.-L. Birck, S. Moorbath, ^{146}Sm-^{142}Nd evidence from Isua metamorphosed sediments for early differentiation of the Earth's mantle. *Nature* **423**, 428–432 (2003).
7. L. E. Borg, J. N. Connelly, M. Boyet, R. W. Carlson, Chronological evidence that the Moon is either young or did not have a global magma ocean. *Nature* **477**, 70–72 (2011).
8. L. E. Borg, G. A. Brennecka, S. J. K. Symes, Accretion timescale and impact history of Mars deduced from the isotopic systematics of martian meteorites. *Geochim. Cosmochim. Acta* **175**, 150–167 (2014).
9. L. E. Borg *et al.*, Isotopic evidence for a young lunar magma ocean. *Earth Planet. Sci. Lett.* **523**, 115706 (2019).
10. M. Lugaro *et al.*, Origin of the p-process radionuclides ^{92}Nb and ^{146}Sm in the early Solar System and inferences on the birth of the Sun. *Proc. Natl. Acad. Sci. U.S.A.* **113**, 907–912 (2016).
11. M. Nurmia, G. Graeffe, K. Valli, J. Aaltonen, *Alpha Activity of Sm-146* (University of Helsinki, 1964).
12. A. M. Friedman *et al.*, Alpha decay half lives of ^{148}Gd ^{150}Gd and ^{146}Sm. *Radiochim. Acta* **5**, 192–194 (1966).
13. F. Meissner, W. D. Schmidt-Ott, L. Ziegeler, Half-life and α-ray energy of ^{146}Sm. *Z. Phys. A At. Nucl.* **327**, 171–174 (1987).
14. N. Kinoshita *et al.*, A shorter ^{146}Sm half-life measured and implications for ^{146}Sm-^{142}Nd chronology in the solar system. *Science* **335**, 1614–1617 (2012).
15. I. M. Villa *et al.*, IUPAC-IUGS recommendation on the half-lives of ^{147}Sm and ^{146}Sm. *Geochim. Cosmochim. Acta* **285**, 70–77 (2020).
16. M. E. Sanborn, R. W. Carlson, M. Wadhwa, ^{147,146}Sm–^{143,142}Nd, ^{176}Lu–^{176}Hf, and ^{87}Rb–^{87}Sr systematics in the angrites: Implications for chronology and processes on the angrite parent body. *Geochim. Cosmochim. Acta* **171**, 80–99 (2015).
17. N. E. Marks, L. E. Borg, I. D. Hutcheon, B. Jacobsen, R. N. Clayton, Samarium–neodymium chronology and rubidium–strontium systematics of an Allende calcium–aluminum-rich inclusion with implications for ^{146}Sm half-life. *Earth Planet. Sci. Lett.* **405**, 15–24 (2014).
18. B. Jacobsen *et al.*, ^{26}Al-^{26}Mg and ^{207}Pb-^{206}Pb systematics of Allende CAIs: Canonical solar initial 26Al/27Al ratio reinstated. *Earth Planet. Sci. Lett.* **272**, 353–364 (2008).
19. A. Bouvier, M. Wadhwa, The age of the Solar System redefined by the oldest Pb-Pb age of a meteoritic inclusion. *Nat. Geosci.* **3**, 637–641 (2010).
20. J. N. Connelly *et al.*, The absolute chronology and thermal processing of solids in the solar protoplanetary disk. *Science* **338**, 651–655 (2012).
21. A. Bouvier, M. Boyet, Primitive solar system materials and Earth share a common initial $^{(142)}$Nd abundance. *Nature* **537**, 399–402 (2016).
22. C. Burkhardt *et al.*, A nucleosynthetic origin for the Earth's anomalous $^{(142)}$Nd composition. *Nature* **537**, 394–398 (2016).
23. J.-A. Barrat *et al.*, A 4,565-My-old andesite from an extinct chondritic protoplanet. *Proc. Natl. Acad. Sci. U.S.A.* **118**, e2026129118 (2021).
24. R. Fukai, T. Yokoyama, Neodymium isotope heterogeneity of ordinary and carbonaceous chondrites and the origin of non-chondritic ^{142}Nd compositions in the Earth. *Earth Planet. Sci. Lett.* **474**, 206–214 (2017).
25. R. Fukai, T. Yokoyama, Nucleosynthetic Sr–Nd isotope correlations in chondrites: Evidence for nebular thermal processing and dust transportation in the early Solar System. *Astrophys. J.* **879**, 79 (2019).
26. P. Frossard, Z. Guo, M. Spencer, M. Boyet, A. Bouvier, Evidence from achondrites for a temporal change in Nd nucleosynthetic anomalies within the first 1.5 million years of the inner solar system formation. *Earth Planet. Sci. Lett.* **566**, 116968 (2021).
27. Bouvier *et al.*, The Lu–Hf and Sm–Nd isotopic composition of CHUR: Constraints from unequilibrated chondrites and implications for the bulk composition of terrestrial planets. *Earth Planet. Sci. Lett.* (2008).
28. I. R. Fletcher, K. J. R. Rosman, Precise determination of initial εNd from Sm-Nd isochron data. *Geochim. Cosmochim. Acta* **46**, 1983–1987 (1982).
29. T. L. Norris, A. J. Gancarz, D. J. Rokop, K. W. Thomas, Half-life of ^{26}Al. *J. Geophys. Res.* **88**, B331–B333 (1983).
30. E. J. Catanzaro, T. J. Murphy, E. L. Garner, W. R. Shields, Absolute isotopic abundance ratios and atomic weight of magnesium. *J. Res. Natl. Bur. Stand., A Phys. Chem.* **70A**, 453–458 (1966).
31. J. A. Van Orman, D. J. Cherniak, N. T. Kita, Magnesium diffusion in plagioclase: Dependence on composition, and implications for thermal resetting of the ^{26}Al-^{26}Mg early solar system chronometer. *Earth Planet. Sci. Lett.* **385**, 79–88 (2014).

32. X. Zhang, J. Ganguly, M. Ito, Ca–Mg diffusion in diopside: Tracer and chemical inter-diffusion coefficients. *Contrib. Mineral. Petrol.* **159**, 175–186 (2010).

33. T. Gregory, T.-H. Luu, C. D. Coath, S. S. Russell, T. Elliott, Primordial formation of major silicates in a protoplanetary disc with homogeneous $^{26}Al/^{27}Al$. *Sci. Adv.* **6**, eaay9626 (2020).

34. J. Bollard *et al.*, Combined U-corrected Pb-Pb dating and ^{26}Al-^{26}Mg systematics of individual chondrules – Evidence for a reduced initial abundance of ^{26}Al amongst inner Solar System chondrules. *Geochim. Cosmochim. Acta* **260**, 62–83 (2019).

35. M. Schiller, J. N. Connelly, A. C. Glad, T. Mikouchi, M. Bizzarro, Early accretion of protoplanets inferred from a reduced inner solar system ^{26}Al inventory. *Earth Planet. Sci. Lett.* **420**, 45–54 (2015).

36. A. Trinquier, J. L. Birck, C. J. Allegre, Widespread ^{54}Cr Heterogeneity in the Inner Solar System. *Astrophys. J.* **655**, 1179–1185 (2007).

37. P. H. Warren, Stable isotopes and the noncarbonaceous derivation of ureilites, in common with nearly all differentiated planetary materials. *Geochim. Cosmochim. Acta* **75**, 6912–6926 (2011).

38. J. A. Barrat *et al.*, Evidence from Tm anomalies for non-CI refractory lithophile element proportions in terrestrial planets and achondrites. *Geochim. Cosmochim. Acta* **176**, 1–17 (2016).

39. T. S. Kruijer, T. Kleine, L. E. Borg, The great isotopic dichotomy of the early Solar System. *Nat. Astron.* **4**, 32–40 (2020).

40. N. S. Saji, D. Wielandt, J. C. Holst, M. Bizzarro, Solar system Nd isotope heterogeneity: Insights into nucleosynthetic components and protoplanetary disk evolution. *Geochim. Cosmochim. Acta* **281**, 135–148 (2020).

41. J. Render, G. A. Brennecka, Isotopic signatures as tools to reconstruct the primordial architecture of the Solar System. *Earth Planet. Sci. Lett.* **555**, 116705 (2021).

42. M. Boyet, R. W. Carlson, A highly depleted moon or a non-magma ocean origin for the lunar crust? *Earth Planet. Sci. Lett.* **262**, 505–516 (2007).

43. A. D. Brandon *et al.*, Re-evaluating $^{142}Nd/^{144}Nd$ in lunar mare basalts with implications for the early evolution and bulk Sm/Nd of the Moon. *Geochim. Cosmochim. Acta* **73**, 6421–6445 (2009).

44. C. L. McLeod, A. D. Brandon, R. M. G. Armytage, Constraints on the formation age and evolution of the Moon from ^{142}Nd–^{143}Nd systematics of Apollo 12 basalts. *Earth Planet. Sci. Lett.* **396**, 179–189 (2014).

45. V. Debaille, A. D. Brandon, Q. Z. Yin, B. Jacobsen, Coupled ^{142}Nd-^{143}Nd evidence for a protracted magma ocean in Mars. *Nature* **450**, 525–528 (2007).

46. G. Caro, B. Bourdon, A. N. Halliday, G. Quitté, Super-chondritic Sm/Nd ratios in Mars, the Earth and the Moon. *Nature* **452**, 336–339 (2008).

47. T. S. Kruijer *et al.*, The early differentiation of Mars inferred from Hf-W chronometry. *Earth Planet. Sci. Lett.* **474**, 345–354 (2017).

48. R. M. G. Armytage, V. Debaille, A. D. Brandon, C. B. Agee, A complex history of silicate differentiation of Mars from Nd and Hf isotopes in crustal breccia NWA 7034. *Earth Planet. Sci. Lett.* **502**, 274–283 (2018).

49. M. Boyet, R. W. Carlson, M. Horan, Old Sm–Nd ages for cumulate eucrites and redetermination of the solar system initial $^{146}Sm/^{144}Sm$ ratio. *Earth Planet. Sci. Lett.* **291**, 172–181 (2010).

50. P. Vermeesch, R. Isoplot, A free and open toolbox for geochronology. *Geoscience Frontiers* **9**, 1479–1493 (2018).

51. N. E. Marks, L. E. Borg, C. K. Shearer, W. S. Cassata, Geochronology of an Apollo 16 clast provides evidence for a basin-forming impact 4.3 billion years ago. *J. Geophys. Res. Planets* **124**, 2465–2481 (2019).

52. J. O'Neil, H. Rizo, M. Boyet, R. W. Carlson, M. T. Rosing, Geochemistry and Nd isotopic characteristics of Earth's Hadean mantle and primitive crust. *Earth Planet. Sci. Lett.* **442**, 194–205 (2016).